ELSEVIER

S0032-3861(96)00351-5

Polymer Vol. 37 No. 23, pp. 5179–5187, 1996
Copyright © 1996 Elsevier Science Ltd
Printed in Great Britain. All rights reserved
0032-3861/96/$15.00+0.00

Cocrystallization of poly(vinylidene fluoride) and vinylidene fluoride–tetrafluoroethylene copolymers:
2. Thermodynamic study

Jhunu Datta and Arun K. Nandi*
Polymer Science Unit, Indian Association for the Cultivation of Science, Jadavpur, Calcutta 700 032, India
(Received 29 November 1994; revised 13 November 1995)

The phase diagrams of poly(vinylidene fluoride) (PVF_2; KF and KY) and vinylidene fluoride–tetrafluoroethylene (VF_2–VF_4) copolymers (Cop-1, Cop-2) have been reported. They are the KF/KY, Cop-1/Cop-2, KF/Cop-1 and KY/Cop-1 systems. The head to head (H–H) defect structures of KF, KY, Cop-1 and Cop-2 are 3.5, 5.3, 15.8 and 21.3 mol%, respectively. The KF/KY and Cop-1/Cop-2 blends exhibit linear variation of apparent melting points with composition but the KF/Cop-1 and KY/Cop-1 blends show a bifurcation of melting point–composition diagram at the Cop-1 rich regions. The crystallization temperature (T_c)–composition plots are linear except for the KF/Cop-1 system. The anomaly of the KY/Cop-1 system in this regard has been explained. The equilibrium melting points (T_m^0) of the blends were determined using the Hoffman–Weeks procedure. The KF/KY blends show a slightly concave upward T_m^0 vs. composition curve indicating weak interaction of the components. The Cop-1/Cop-2 blends exhibit a linear plot over the same composition due to ideal mixing. Both the KF/Cop-1 and KY/Cop-1 blends exhibit a concave upward curve with some concave downward portion for the T_m^0 vs. composition plots at the Cop-1 rich regions. Further, at the Cop-1 rich regions ($W_{\text{Cop-1}} = 0.75$), three melting peaks of isothermally crystallized KF/Cop-1 and KY/Cop-1 blends were observed when melted from the T_cs. Liquid–liquid phase separation in the melt for the KF/Cop-1 and KY/Cop-1 systems at Cop-1 rich compositions has been attributed to the different behaviour rather than observed from the other pairs. The cocrystallization of this system is complicated by both the crystalline phase segregation and the liquid–liquid phase segregation. Copyright © 1996 Elsevier Science Ltd.

(Keywords: PVF_2; VF_2–VF_4 copolymers; phase diagrams)

INTRODUCTION

Recently, crystalline polymer blends have been intensively investigated from the viewpoint of cocrystallization. They are the blends of polyethylene of different commercial grades[1–5], poly(vinyl fluoride) and poly(vinylidene fluoride)[6,7], vinylidene fluoride–trifluoroethylene (VF_2–VF_3) copolymers[8], poly(tetrafluoroethylene) and poly(tetrafluoroethylene-*co*-perfluoroalkyl-vinyl ether)[9], etc. However, there is a lack of complete thermodynamic studies in most of these systems. In this paper we present a thermodynamic study of such a system using poly(vinylidene fluoride) (PVF_2) and vinylidene fluoride–tetrafluoroethylene (VF_2–VF_4) copolymers.

Both PVF_2 and VF_2–VF_4 copolymers contain different amounts of head to head (H–H)/pseudo head to head defect structure in their chain[10,11]. Earlier we had established the cocrystallization possibilities among the different defect content samples and also reported the influence of crystallization temperature on the cocrystallization of the above polymers at the 1/1 composition of the mixture[12]. It was established from these studies that cocrystallization of PVF_2 and VF_2–VF_4 copolymer is limited to the difference of 12 mol% H–H defect structure in the chains of the two components. In order to understand the cocrystallization process of these polymers more explicitly we studied the phase diagrams of the mixtures and determined the results presented here.

The phase diagrams (melting point–composition plots) of binary mixtures of crystalline polymers (miscible in melt) are generally of four different types[8]: (a) immiscible with eutectic; (b) immiscible with no eutectic; (c) miscible with concave upward (weak interaction); and (d) miscible with concave downward (strong interaction). Tanaka *et al.* studied the phase diagrams of the blends of vinylidene fluoride–trifluoroethylene (VF_2–VF_3) copolymers and observed that they belonged to type II and type III classes depending upon the difference of co-unit concentration of the components[8]. Keller and his co-workers made extensive studies of the phase diagrams of linear polyethylene (LPE) with branched polyethylene (BPE) and observed that they did not produce cocrystals at all compositions[4,13,14]. From both the d.s.c. and morphology studies they concluded that the blends of BPE rich regions are biphasic in nature and

---

[*] To whom correspondence should be addressed

attributed it to the liquid–liquid phase separation of the melt at this composition. However, in a recent paper, Alamo *et al.* reported from small angle neutron scattering studies that there is no liquid–liquid phase separation in this system and the biphasic nature of the blend is due to the crystallization process[15]. These contradictory reports on the cocrystallization mechanism of this system needs to be studied in other systems. PVF_2 and VF_2–VF_4 copolymers are an ideal pair in this regard and a thermodynamic study may help to delineate the mechanism of cocrystallization in this system.

EXPERIMENTAL

The characteristics of the samples used in the work are presented in *Table 1*[12]. Pairs of these polymers were mixed in different composition by dissolving in *N*,*N*-dimethyl formamide at 80°C followed by evaporation of the solvent at 60°C. They were finally dried at 70°C for 3 days. Here it is necessary to mention that the KF and KY PVF_2 crystallizes in the α phase whereas the Cop-1 and Cop-2 crystallize in the β phase when crystallized from the melt[12].

In the thermodynamic study we choose the experiments in three different directions: (a) measurement of the apparent melting points of the blends crystallized at different temperatures; (b) measurement of the crystallization temperatures (T_c) of the blends crystallized from the melt at a cooling rate of $2.5° \min^{-1}$; and (c) measurement of the equilibrium melting points of the blends. In the first set of experiments the apparent melting points of the whole composition of the blends are reported from crystallization at three different crystallization temperatures, e.g. (a) at 50°C, (b) at 120°C and (c) at 135°C. For crystallization at 50°C about 5 mg of the samples were used and melted at 227°C in the d.s.c. for 10 min. They were then quenched at $200°\mathrm{C} \min^{-1}$ to 50°C and kept for 10 min before starting the melting run. The crystallization at 120°C and 135°C were carried out by sealing the d.s.c. capsules in glass tubes under vacuum (10^{-4} torr). They were melted in a thermostatic bath set at 227°C for 10 min and quickly transferred to another bath set at the predetermined crystallization temperature. Sufficient time for crystallization was given in each case and in each series of blends the same time of crystallization has been given so that comparison can be done fruitfully. KF and KY PVF_2 samples exhibit melt recrystallization[16,17] and to eliminate the melt recrystallization of their blends they were crystallized for five days at both temperatures. The melting of the cocrystals was studied in a Perkin-Elmer DSC-7 equipped with 3700 data station at the heating rate of $10° \min^{-1}$. The instrument was calibrated with indium before use. The peak temperatures were taken as the melting points.

The measurement of crystallization temperatures (T_c) were carried out by the dynamic cooling method. The samples were melted at 227°C and cooled at $2.5° \min^{-1}$ and the exotherms were recorded. The exothermic peak temperature was taken as T_cs.

For the measurement of equilibrium melting points isothermal crystallizations were performed by melting the samples at 227°C and then rapidly quenched to the predetermined isothermal crystallization temperature. After crystallization for different times they were heated from this temperature at $10° \min^{-1}$ without cooling. The peak melting temperatures were plotted against crystallinity and the melting points at 10% crystallinity was taken as a measure of T_m at each T_c. The melting points of the α and β phases (where it was produced) only were considered here. No melting study on γ and γ' phases was made.

RESULTS AND DISCUSSION

Apparent melting points

In *Figure 1(a–d)* the melting endotherms are shown for the samples crystallized at 120°C. In *Figure 1a* the endothermic peaks are very sharp for all compositions indicating that KF and KY PVF_2 have cocrystallized at this temperature over the whole composition range. The melting endotherms of Cop-1/Cop-2 blends (*Figure 1b*) are broader than those of the earlier pair but it is apparent from the figure that co-crystallization is taking place for all compositions because the characteristic higher melting peak of Cop-2 is absent in the blends. In *Figure 1c* the melting endotherms of KY/Cop-1 blends are presented. From the figure it is clear that the endothermic peaks are broader with increasing Cop-1 content and at $W_{\mathrm{Cop\text{-}1}} = 0.68$ and 0.72 the two peaks of the components are clearly resolved indicating no cocrystallization at these compositions. However, at $W_{\mathrm{Cop\text{-}1}} = 0.95$ no multiplicity of the melting peak is found indicating complete co-crystallization at this composition. In *Figure 1d* melting endotherms of the KF/Cop-1 system are presented. Here also, with increasing Cop-1 concentration in the blend, the peaks became broader and at $W_{\mathrm{Cop\text{-}1}} = 0.74$ and 0.93 multiplicity in the melting peaks was observed. Thus at these two compositions co-crystallization does not take place. From these results it is apparent that if the difference of H–H defect concentration of the components increases cocrystallization is less favoured and with increasing concentration of the higher H–H defect component in the blend the situation also becomes worse.

To understand the effect of crystallization temperature on the cocrystallization process we studied the systems by crystallizing at two other temperatures. In *Figures 2a* and *b* typical melting endotherms of KF/Cop-1 blends

Table 1 Characteristics of the PVF_2 and (VF_2–VF_4) copolymer samples

Sample	$\bar{M}_w \times 10^{-5}$	PDI	VF_4 content (mol%)	H–H defect (mol%)	Polymorph
KF	4.28	1.47	0.00	3.5	α
KY	7.36	2.04	0.00	5.31	α
Cop-1	1.97	2.07	9.1	15.8	β
Cop-2	3.23	2.63	14.3	21.3	β

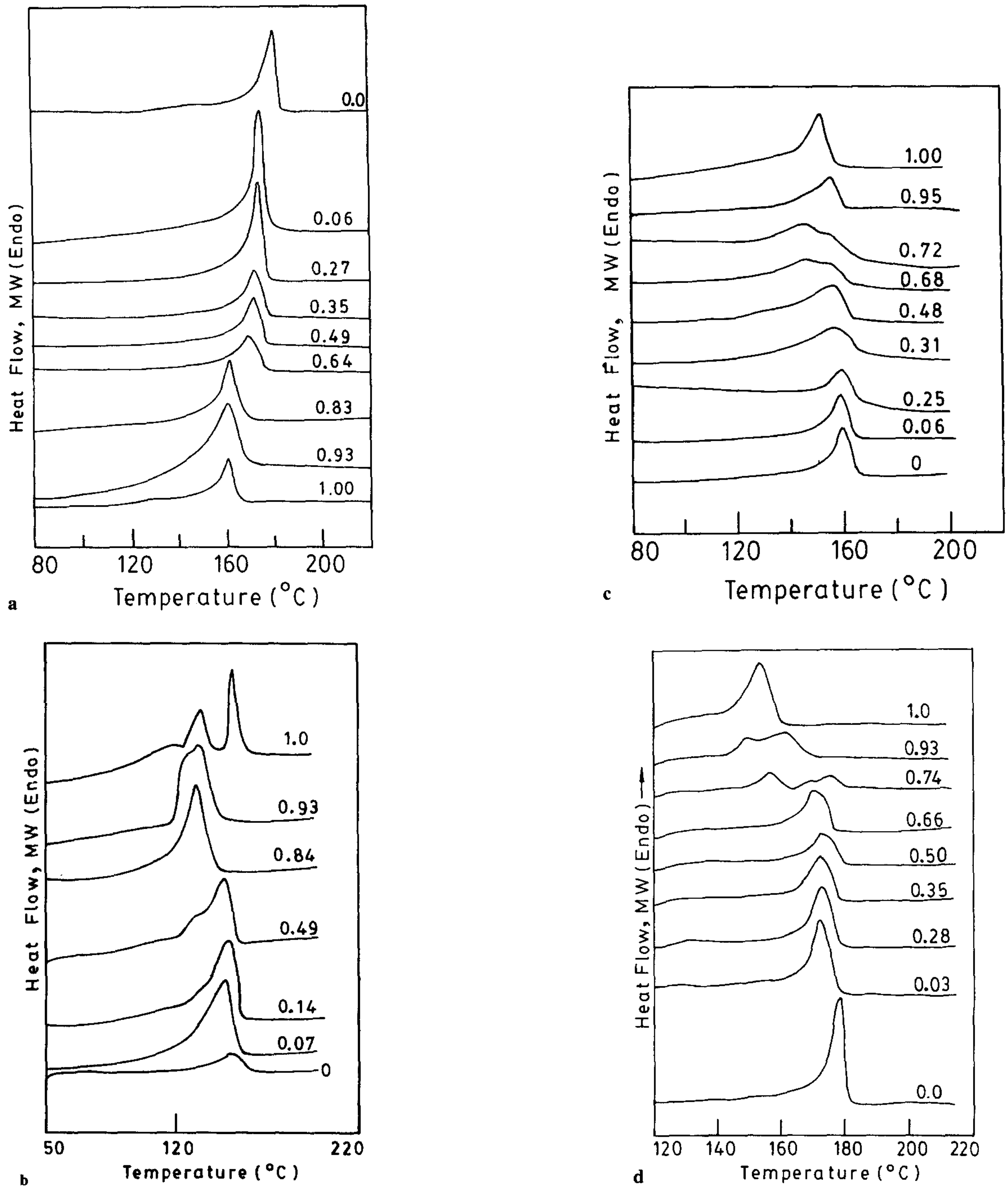

Figure 1 (a) Melting endotherms of KF/KY blends crystallized at 120°C for 5 days at the indicated weight fractions of KY PVF$_2$. (b) Melting endotherms of Cop-1/Cop-2 blends crystallized at 120°C for one day at the indicated weight fractions of Cop-2. (c) Melting endotherms of KY/Cop-1 blends crystallized at 120°C for five days at the indicated weight fractions of Cop-1. (d) Melting endotherms of KF/Cop-1 blends crystallized at 120°C for five days at the indicated weight fraction of Cop-1

are presented for samples crystallized at 50°C and 135°C respectively. In *Figure 2a* the melting endotherms of KF/Cop-1 blends crystallized at 50°C are shown. It is apparent from the figure that for the blends of compositions $W_{\mathrm{Cop\text{-}1}} \geq 0.5$ two melting peaks are observed, the lower correspond to the melting of Cop-1 and the higher for that of KF. For compositions $W_{\mathrm{Cop\text{-}1}} < 0.5$ two peaks are observed in some cases, however, none of these correspond to melting of Cop-1 and this indicates that the blends of compositions $W_{\mathrm{Cop\text{-}1}} < 0.5$ are producing cocrystals. The double peaks at compositions $W_{\mathrm{Cop\text{-}1}} < 0.5$, therefore, arise due to the melt-recrystallization and the melt recrystallization vanishes for crystallization at 120°C (*Figure 1b*) for five days. In *Figure 2b* the melting endotherms of the samples crystallized at 135°C are shown. From the figure, it is clear that there are multiple melting peaks of blends having compositions $W_{\mathrm{Cop\text{-}1}} \geq 0.28$. Two melting peaks (at 142°C and at 173°C) are clearly seen in the blends with one intermediate shoulder at ~155°C in some cases. These 142° peaks were absent for crystallization at 50° and also at 120°C. The melting point of Cop-1 (crystallized at 135°C) is 155°C, so the reason for such a low temperature peak at ~142°C may be due to a fraction of the Cop-1 having very high H–H defect concentration. Such a fractionation process during crystallization is quite possible because the temperature 135°C is the isothermal

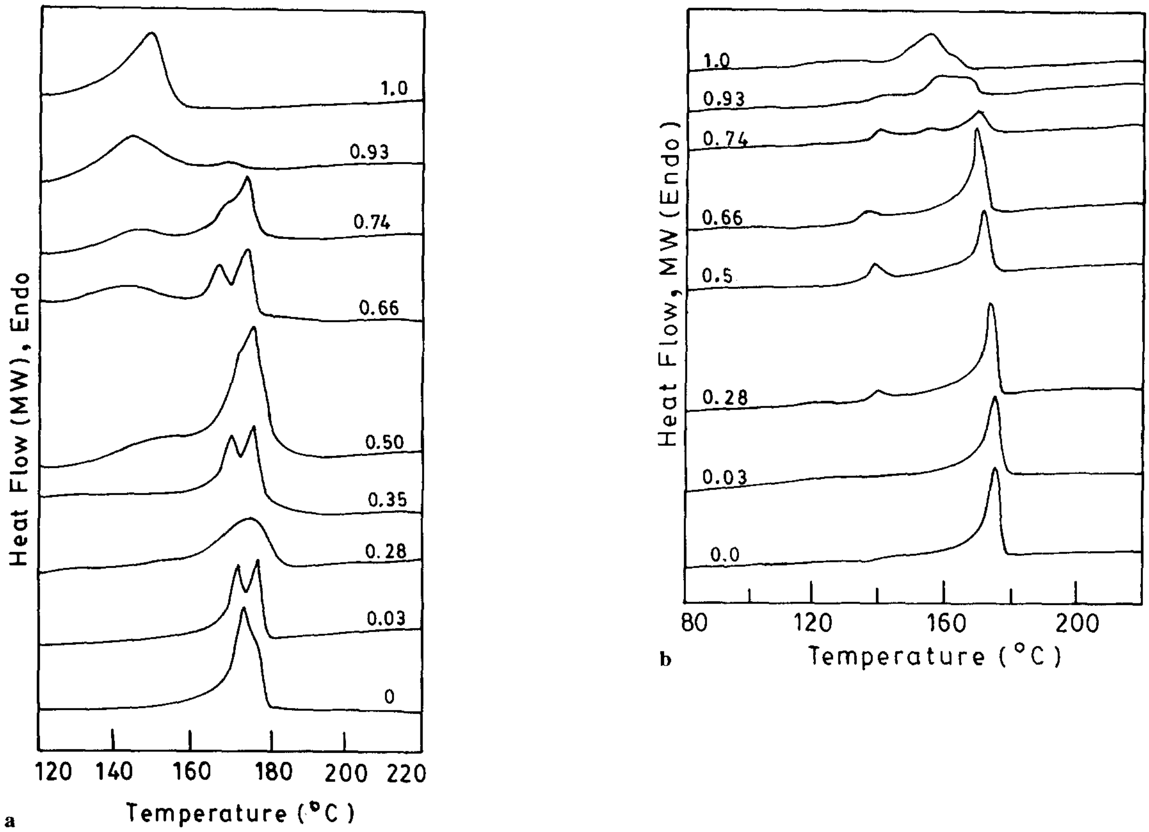

Figure 2 (a) Melting endotherms of KF/Cop-1 blends quenched at 50°C at the indicated weight fraction of Cop-1. (b) Melting endotherms of KF/Cop-1 blends crystallized at 135°C for five days at the indicated weight fraction of Cop-1

region for crystallization of Cop-1 and the undercooling difference of the two components is very large (40°). The lower defect content fraction of Cop-1 produces co-crystal with KF except the compositions 0.74 and 0.93 where three melting peaks are clearly observed. In the KY/Cop-1 system this type of phase segregation is not favoured because the undercooling difference of the two components is smaller (16°).

To delineate completely the influence of temperature on the cocrystallization behaviour of these systems the phase diagrams are drawn in *Figures 3a–d*. In these phase diagrams the apparent melting points (T_m) are plotted against the composition of blends crystallized at different temperatures. The equilibrium melting point (T_m^0) of the cocrystals are also presented in these diagrams and will be discussed later. In *Figures 3a* and *b* the KF/KY and Cop-1/Cop-2 blends exhibit a linear dependency between the apparent melting points of the parent components with composition. However, in *Figures 3c* and *d* the melting point composition diagrams are of a different type than those of the former systems. In the KY/Cop-1 system (*Figure 3c*) cocrystals are not produced over the whole composition of the blend in any of the crystallization temperatures studied. There is a bifurcated area in the figure at each crystallization temperature and it represents the immiscibility in the solid state at these blend compositions. In *Figure 3d* similar but larger bifurcated areas have been observed indicating greater immiscibility of the KF/Cop-1 system than the KY/Cop-1 system. The reason for the larger immiscibility in the KF/Cop-1 system compared to that of the KY/Cop-1 system may be due to the larger difference in defect concentration in the former than that in the latter pair. One interesting observation in this system is that the immiscibility area at first decreases with increase in crystallization temperature to 120°C and after that it again increases with increase in crystallization temperature to 135°C. The reason is yet uncertain and a probable cause for the decrease of the immiscibility area with increase in temperature may be due to the easier incorporation of H–H defect in the crystalline lamella at higher temperature producing cocrystal[12]. Support of this assertion comes from the fact that d_{hkl} of both the α and β phases of PVF_2 increases with increase in T_c and this possibly occurs due to the incorporation of larger size H–H defect in the lamella[18] in greater numbers. The increase of immiscibility area at 135°C is due to the segregation of higher defect content fractions during crystallization from the melt as stated earlier.

Crystallization temperatures

The composition dependence of the crystallization temperatures (T_cs) of each blend has been presented in *Figure 4*. Single T_c offers secondary evidence of cocrystallization and have certain limitations as discussed below. In the figure KF/KY, Cop-1/Cop-2 and KY/Cop-1 systems exhibit linear plots of T_c with composition, whereas the KF/Cop-1 system shows bifurcation which suggests that they are not producing cocrystals at all compositions. It has been pointed out earlier that KF/KY and Cop-1/Cop-2 cocrystallize over the whole composition range. However, in the case of the KY/Cop-1 system there is some doubt. The exotherms of this system presented in *Figure 5*, are similar to those of the other cocrystal pairs. In *Figure 6* the melting

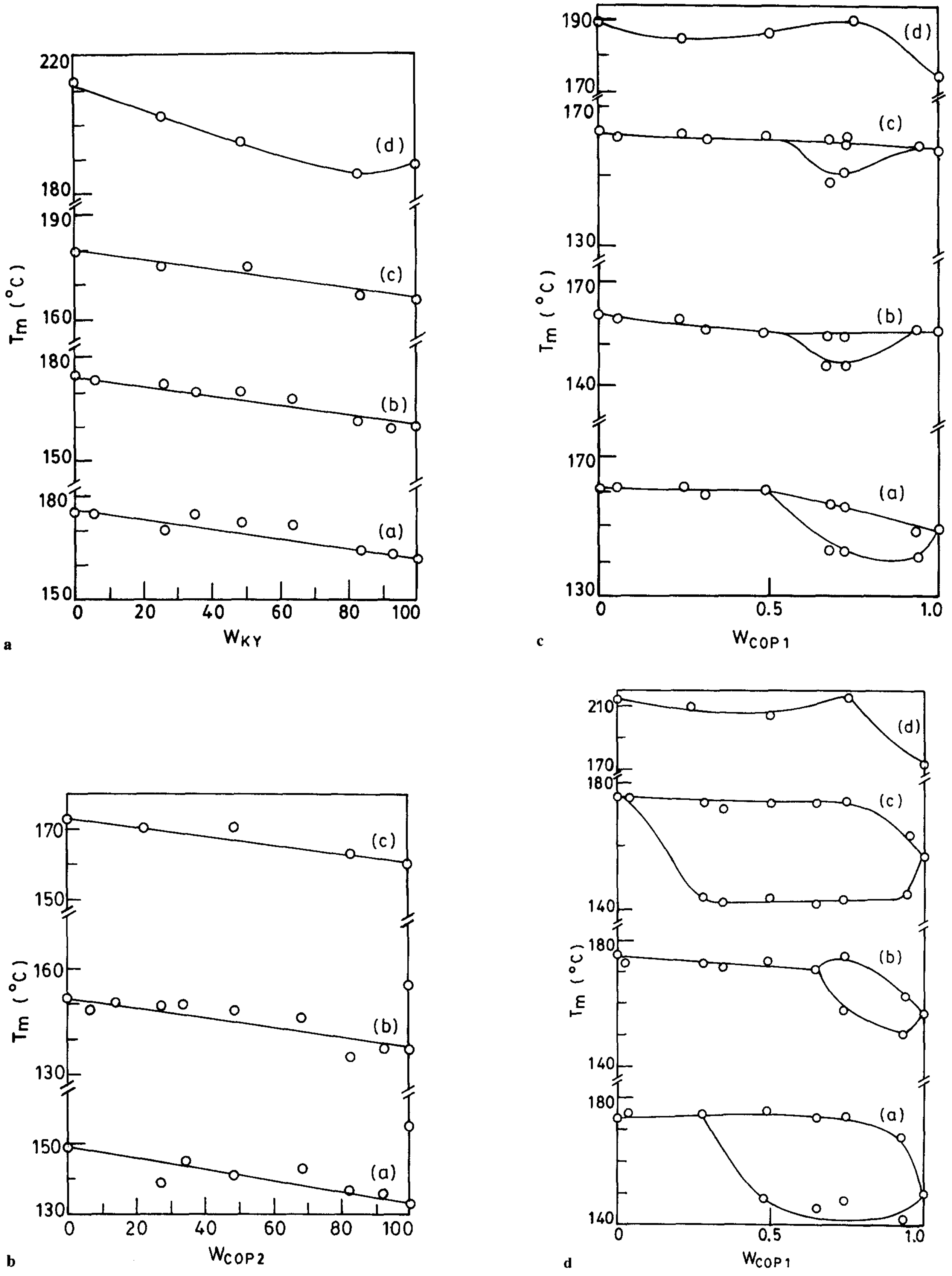

Figure 3 (**a**) Phase diagrams of KF/KY PVF_2 blends crystallized at (a) 50°C, (b) 120°C, (c) 135°C and (d) equilibrium melting points. (**b**) Phase diagrams of Cop-1/Cop-2 blends crystallized at (a) 50°C, (b) 120°C and (c) equilibrium melting points. (**c**) Phase diagrams of KY/Cop-1 blends crystallized at (a) 50°C, (b) 120°C, (c) 135°C and (d) equilibrium melting points. (**d**) Phase diagrams of KF/Cop-1 blends crystallized at (a) 50°C, (b) 120°C, (c) 135°C and (d) equilibrium melting points

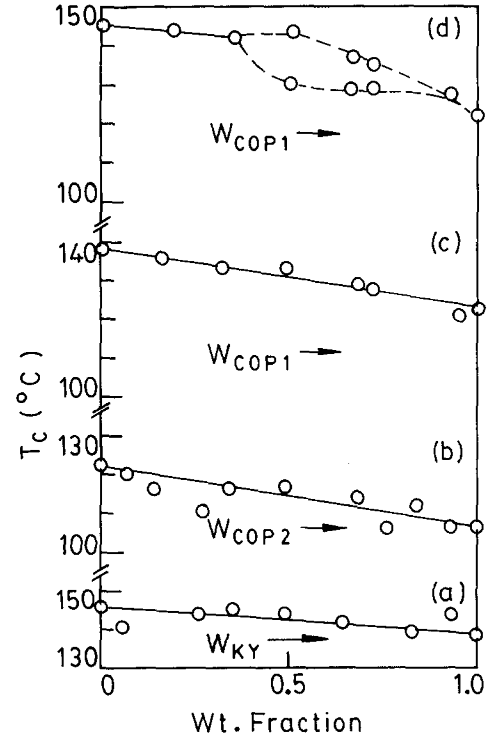

Figure 4 T_c composition plots of (a) KF/KY, (b) Cop-1/Cop-2, (c) KY/Cop-1 and (d) KF/Cop-1 blends obtained from cooling the melt (227°C) at the rate of 2.5° min^{-1}

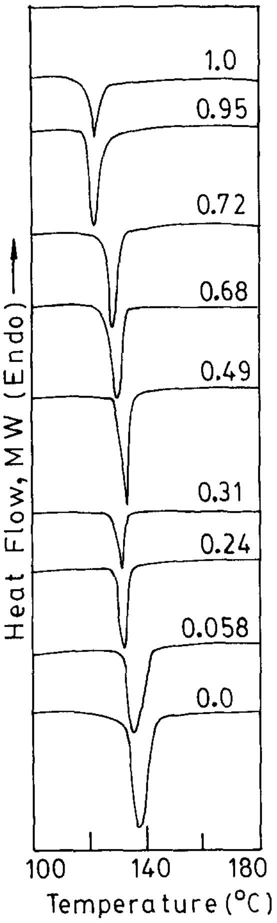

Figure 5 Crystallization exotherms of KY/Cop-1 blends obtained from cooling the melt (227°C) at the rate of 2.5° min^{-1} for the indicated weight fraction of Cop-1

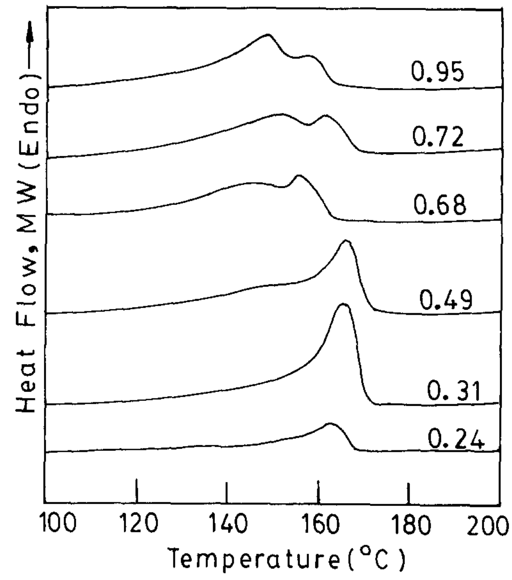

Figure 6 Melting endotherms of KY/Cop-1 blends crystallized as in *Figure 5* at the indicated weight fraction of Cop-1

endotherms of KY/Cop-1 blends crystallized by the above procedure are presented. From the figure it is clear that for compositions $W_{\text{Cop-1}} > 0.5$ the blends exhibit two peaks while for the composition $W_{\text{Cop-1}} < 0.5$ they exhibit a single peak. Thus it may be concluded that KY/Cop-1 blends with $W_{\text{Cop-1}} > 0.5$ are not producing cocrystals though they exhibit a single peak in the crystallization exotherms. The T_cs of the KY PVF_2 and Cop-1 differ by 15° and is 8° less than that of the KF/Cop-1 system and it may be a cause to exhibit a single exotherm at Cop-1 rich blends of the KY/Cop-1 system. Thus the phase diagram based on crystallization temperature are less important compared to those based on melting temperature.

Equilibrium melting point

This section is much more important because it not only represents the characteristics of the crystalline state but it also reflects the thermodynamics of the liquid state in the melt. The equilibrium melting points were determined using Hoffman–Weeks procedure[19] taking the melting points as the same and low level of crystallinity (10%) of the blend at each crystallization temperature[16,20]. Here it is necessary to mention that equilibrium melting points of α phase of PVF_2 and those of the β phase of copolymers were determined. The equilibrium melting points of the γ phase were not determined though it occurred in some PVF_2 blends.

In *Figure 7* the Hoffmann–Weeks plots of KF/KY, Cop-1/Cop-2 and KY/Cop-1 blends are shown for their 1/1 composition. As in the pure PVF_2 the plots of KF/KY and KY/Cop-1 systems show a break at lower crystallization temperature. The reason is the same as discussed earlier[16,20]. However, it may be pointed out that Cop-1, Cop-2 and their blends do not exhibit such a break in any of the composition. The equilibrium melting points and slopes of the upper portions of Hoffman–Weeks plots are presented in *Table 2*. The slope values are close to the theoretical value of 0.5 and are similar to the values reported earlier[16,20].

Some interesting thermograms of KY/Cop-1 blends at

Table 2 Equilibrium melting points and slopes of Hoffman–Weeks plot of PVF_2 and VF_2–VF_4 copolymer blends

Blend	Composition[a]	Polymorph	Slope	$T_m^0 \pm 2$(°C)
KF/KY	0.0	α	0.72	213
	1.0	α	0.69	189
	0.25	α	0.71	202
	0.50	α	0.67	197.4
	0.75	α	0.58	186
Cop-1/Cop-2	0.0	β	0.44	173
	1.0	β	0.43	159
	0.25	β	0.46	172
	0.50	β	0.41	171
	0.75	β	0.38	162
KY/Cop-1	0.25	α	0.57	184
	0.50	α	0.59	185.6
	0.75	α	0.47	189
KF/Cop-1	0.25	α	0.68	210
	0.50	α	0.58	203
	0.75	α	0.71	213

[a] Weight fraction of higher H–H defect component of the blend

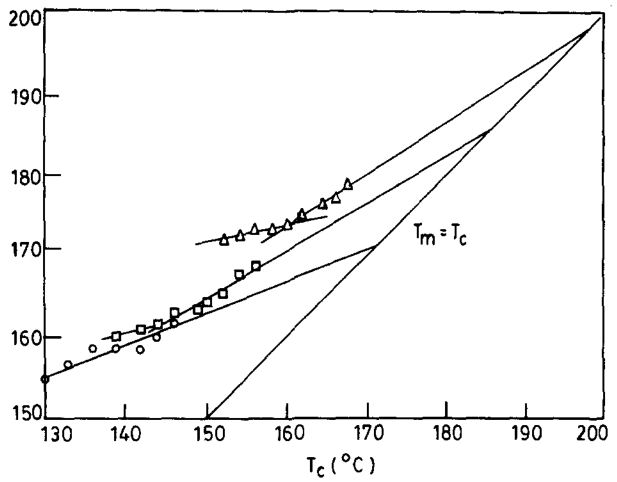

Figure 7 Hoffman–Weeks plots at the 1/1 (by weight) composition of the blends. △, KF/KY; □, KY/Cop-1; ○, Cop-1/Cop-2

composition $W_{\text{Cop-1}} = 0.75$ during melting of isothermally crystallized samples are presented in *Figure 8*. For crystallization at 139°C two peaks (145°C and 166°C) and a hump (160°C) are observed and with increasing crystallization temperature the size of the hump increases to give the shape of a peak and clearly there are three peaks for crystallization at 145°C. With a further increase in T_c the highest temperature peak decreases in size and takes the shape of a hump at 152°C and at 158°C it vanishes showing only two peaks. The KF/Cop-1 system at composition $W_{\text{Cop-1}} = 0.75$ also yields similar thermograms and the highest melting peak vanishes while crystallizing at 168°C. Both the KF and KY PVF_2 can crystallize in the α and γ phases depending on the crystallization temperature, whereas Cop-1 crystallizes only in the β phase. If the components are miscible in the melt then crystallization in any of the α or β polymorphs of PVF_2 takes place according to the resultant H–H defect concentration in the melt[11,18]. The γ polymorph is usually produced at higher temperature and it increases with increase in crystallization temperature[21]. The highest temperature peak is not, therefore, due to the γ phase because the peak area decreases with increase in T_c. To find the origin of the three peaks we made T_m–T_c plots which are shown in *Figure 9*, where the T_m–T_c plots of pure KY and Cop-1 are also presented. From the figure it is apparent that the T_m–T_c line of the lowest melting peak is lower than those of Cop-1 and KY PVF_2, while the T_m–T_c lines of the other two melting peaks are higher than those of Cop-1 and KY PVF_2.

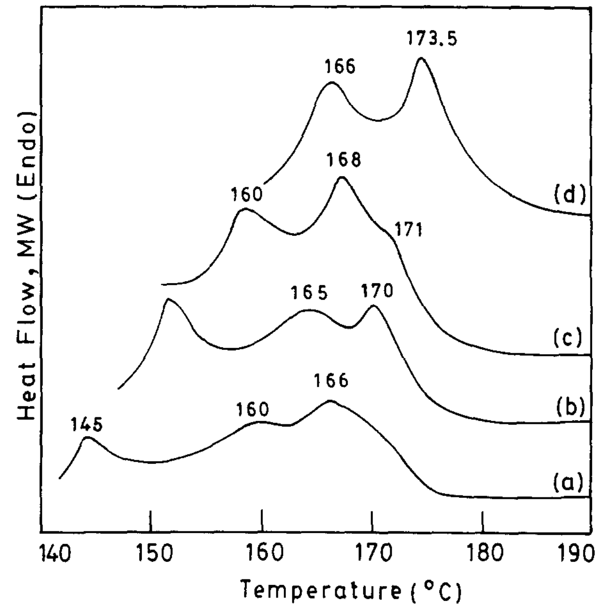

Figure 8 Melting endotherms of isothermally crystallized KY/Cop-1 blend ($W_{\text{Cop-1}} = 0.75$) (10% crystallinity) crystallized at different crystallization temperatures (a) 139°C, (b) 145°C, (c) 152°C and (d) 158°C. The d.s.c. was scanned from the T_c at 10° min^{-1} without cooling

To explain this phenomenon it may be argued that there is structural heterogeneity in both the KY PVF_2[16] and Cop-1 and the highest regular fraction of KY PVF_2 produces the highest melting peak, the lowest regular fraction of Cop-1 produces the lowest melting peak and the lower regular fraction of KY and the higher regular fraction of Cop-1 produces the middle melting peak. The apparent melting points conform to such a fractionation process. But how does such a fractionation occur? It is possible in two ways: (a) liquid–liquid phase separation; and (b) liquid–crystal phase separation. The latter possibility can be ignored because the highest melting peak gradually decreases with increasing T_c and vanishes when crystallized at 158°C. If it is fractionation due to crystallization the highest temperature peak should be sharper with increasing T_c because fractionation is favoured at higher T_c. Therefore, the fractionation is occurring due to the liquid–liquid phase separation[22] and here it is a three phase system. Although in the ternary systems two phase regions are more common[24], three phase regions are also possible as suggested by Tompa [24,25]. Koningsveld *et al.* observed three phases in binary polymer solvent systems with broader molar mass distribution of the polymer[26,27] and three liquid phases also occurred in the binary blends of linear polyethylene with branched polyethylene[28]. Thus, in the binary system with wider structural heterogeneity, three liquid phases are possible and we can propose that in the binary blends of PVF_2 and VF_2–TFE copolymer three liquid phases produce three crystalline phases which show the three melting peaks during melting. In *Figures 9* and *10* the Hoffman–Weeks plots to obtain T_m^0 of the ternary systems have been shown. There is some difference in two plots. *Figure 9* shows that the lower and middle melting peak cannot be extrapolated to the $T_m = T_c$ line, but the higher melting temperature can be extrapolated to yield T_m^0 value. In the KF/Cop-1 system (*Figure 10*) the situation is different and here the middle peak can be extrapolated to yield a T_m^0 value equal to that of KF but not the others. The cause of difference in extrapolation of the melting peaks of KF/Cop-1 and KY/Cop-1 blends ($W_{Cop\text{-}1} = 0.75$) to $T_m = T_c$ line is not known. A probable reason may be due to the difference in the ternary phase diagrams and also due to the difference in their temperature variation of the last two systems[28]. The same T_m^0 values of the blends to those of pure KF and KY PVF_2 suggest that there is no favourable interaction at this composition of KF/Cop-1 and KY/Cop-1 blends required for mixing[20].

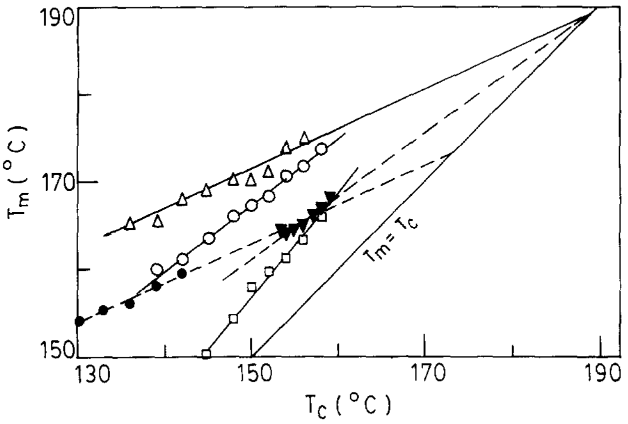

Figure 9 Hoffman–Weeks plots of KY/Cop-1 blend ($W_{Cop\text{-}1} = 0.75$). □, for the lower melting peak; ○, for the middle melting peak; △, for the higher melting peak; ●, for Cop-1; and ▼, for KY[16]

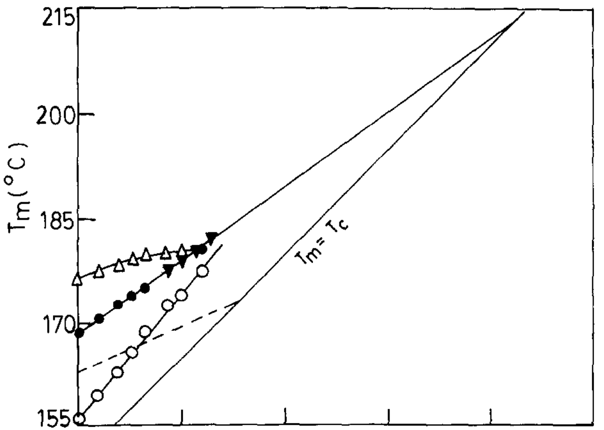

Figure 10 Hoffman–Weeks plots of KF/Cop-1 blend ($W_{Cop\text{-}1} = 0.75$): ○, for the lower melting peak; ●, for the middle peak; △, for the higher melting peak; ▼, data of pure KF[16]; the dotted line indicates the T_m–T_c line of Cop-1

Now we want to discuss the T_m^0–composition plots of the systems (*Figures 3a–d*). The KF/KY blends have a concave upward curve and this indicates that there is weak attraction between the components of the system[8]. However, Cop-1 + Cop-2 blends exhibit a linear plot joining those of the components indicating that mixing is ideal. But with increasing difference in defect concentration of the components the nature of the plot is different having both concave upward and concave downward portions. By analogy to the Gibbs free energy of mixing of binary mixtures[24] we can predict that the concave downward portion is metastable and is liable to phase separation both in the melt as well as in the crystalline state. These T_m^0–composition plots also indicate that the interaction parameter is composition dependent in both the KF/Cop-1 and KY/Cop-1 system and this fulfils the requirement for the formation of a three phase system[27] in the Cop-1 rich regions of KF/Cop-1 and KY/Cop-1 blends.The liquid–liquid phase separation in the melt, therefore, hinders the cocrystallization at $W_{Cop\text{-}1} \sim 0.6$–$0.9$ for KY/Cop-1 blends and at $W_{Cop\text{-}1} \sim 0.7$–$0.95$ for KF/Cop-1 blends.

CONCLUSION

Cocrystallization of PVF_2 is very much dependent on the H–H defect present in the parent components and if the difference is low it can co-crystallize in all the compositions at all the temperatures. But if the difference is large cocrystallization is dependent on the crystallization temperature and also on the composition of the blends. The cocrystallization in some cases is hindered due to the fractionation of higher defect content material during crystallization at high temperature. The crystallization temperature composition data cannot yield a true phase diagram of the system. The cause for not forming a cocrystal of KF/Cop-1 and KY/Cop-1 blends at Cop-1 rich regions is expected due to the liquid–liquid phase separation of the system, and where both binary and ternary phase may be possible. Thus the cocrystallization of PVF_2 and VF_2–VF_4 copolymers is a complex process and it is hindered by both liquid–liquid and liquid–crystal phase segregation processes depending on blend composition and crystallization temperature.

ACKNOWLEDGEMENT

We gratefully acknowledge the Council of Scientific and Industrial Research, New Delhi (grant No. 4(112)/91-EMR.11) for financial support of the work.

REFERENCES

1 Hu, S. R., Kyu, T. and Stein, R. S. *J. Polym. Sci.* 1987, **B25,** 71

2 Alamo, R. G., Flaser, R. H. and Mandelkern, L. *J. Polym Sci.* 1988, **B26,** 2169

3 Martinez Salazer, J., Sanchez Cuesta, M. and Plans, J. *Polymer* 1991 **32,** 2984

4 Hill, M. J., Barham, P. J. and Keller, A. *Polymer* 1992, **33,** 2530

5 Tashiro, K., Izuchi, M., Kobayashi, M. and Stein, R. S. *Macromolecules* 1994, **27,** 1221

6 Natta, G., Allegra, G., Basi, I. W., Sianeri, D., Caporiecio, G. and Torti, E. *J. Polym. Sci.* 1965, **A3,** 4263

7 Guerra, G., Karasz, F. E. and MacKnight, W. J. *Macromolecules* 1986, **19,** 1935

8 Tanaka, H., Lovinger, A. J. and Davis, D. D. *J. Polym. Sci.* 1990, **B28,** 2183

9 Runt, J., Jin, L. and Talibuddin, S. *Macromolecules* 1995, **28,** 2781

10 Lovinger, A. J., in 'Developments in Crystalline Polymer' (Ed. by D. C. Basset), Appl. Sci. Pub., London, 1981, p. 195

11 Farmer, B. L., Hopfinger, A. J. and Lando, J. B. *J. Appl. Phys.* 1972, **43,** 4293

12 Datts, J. and Nandi, A. K. *Polymer* 1994, **35,** 4812

13 Hill, M. J., Barham, P. J., Keller, A. and Rosney, C. C. A. *Polymer* 1991, **32,** 1384

14 Barham, P. J., Hill, M. J., Keller, A. and Rosney, C. C. A. *J. Mater. Sci. Lett.* 1988, **7,** 1271

15 Alamo, R. G., Londono, J. D., Mandelkern, L., Stehling, F. C. and Wignall, G. D. *Macromolecules* 1994, **27,** 411

16 Nandi, A. K. and Mandelkern, L. *J. Polym. Sci.* 1991, **B29,** 1287

17 Prest, W. M. Jr. and Luca, D. J. *J. Appl. Phys.* 1975, **46,** 4136

18 Datta, J. and Nandi, A. K. *Polymer* submitted

19 Hoffman, J. D. and Weeks, J. J. *J. Res. Natl Bur. Stand.* 1962, **66,** 13

20 Maiti, P. and Nandi, A. K. *Macromolecules* 1995, **28,** 8511

21 Lovinger, A. J. *J. Polym. Sci.* 1980, **B18,** 793

22 The direct proof of liquid–liquid phase separation in this system is difficult because of the failure of our optical cloud point measurement technique[20]. This is because the difference of refractive index of the components is too small (~ 0.007)[23] to carry out any meaningful measurement

23 'Polymer Handbook' (Eds J. Brandrup and E. H. Immergut), 2nd Edn, John Wiley, New York, 1975. The refractive index of the copolymer has been calculated assuming the linear combination of the component values on mole fraction basis

24 Tompa, H. 'Polymer Solutions', Butterworths, London, 1956

25 Tompa, H. *Trans. Farad. Soc.* 1949, **45,** 1142

26 Koningsveld, R., Staverman, A. J.; Kolloid, Z. Z. *Polymer* 1967, **31,** 220

27 Koningsveld, R., Kleintjens, L. A. and Schultz, A. R. *J. Polym. Sci.* 1970, **8,** 1261

28 Hill, M. J. and Barham, P. J. *Polymer* 1994, **35,** 1802